Uncoupling of Nucleotide Flipping and DNA Bending by the T4 Pyrimidine Dimer DNA Glycosylase†

Randall K. Walker,‡ Amanda K. McCullough,§ and R. Stephen Lloyd*,§

PerkinElmer Life and Analytical Sciences, Boston, Massachusetts 02118-2512, and Center for Research on Occupational and Environmental Toxicology and Department of Molecular and Medical Genetics, Oregon Health and Science University, Portland, Oregon 97239-3098

Received April 24, 2006; Revised Manuscript Received September 12, 2006

ABSTRACT: Bacteriophage T4 pyrimidine dimer glycosylase (T4-Pdg) is a base excision repair protein that incises DNA at cyclobutane pyrimidine dimers that are formed as a consequence of exposure to ultraviolet light. Cocrystallization of T4-Pdg with substrate DNA has shown that the adenosine opposite the 5′-thymine of a thymine−thymine (TT) dimer is flipped into an extrahelical conformation and that the DNA backbone is kinked 60° in the enzyme−substrate (ES) complex. To examine the kinetic details of the precatalytic events in the T4-Pdg reaction mechanism, investigations were designed to separately assess nucleotide flipping and DNA bending. The fluorescent adenine base analogue, 2-aminopurine (2-AP), placed opposite an abasic site analogue, tetrahydrofuran, exhibited a 2.8-fold increase in emission intensity when flipped in the ES complex. Using the 2-AP fluorescence signal for nucleotide flipping, k_{on} and k_{off} pre-steady-state kinetic measurements were determined. DNA bending was assessed by fluorescence resonance energy transfer using fluorescent donor−acceptor pairs located at the 5′-ends of oligonucleotides in duplex DNA. The fluorescence intensity of the donor fluorophore was quenched by 15% in the ES complex as a result of an increased efficiency of energy transfer between the labeled ends of the DNA in the bent conformation. Kinetic analyses of the bending signal revealed an off rate that was 2.5-fold faster than the off rate for nucleotide flipping. These results demonstrate that the nucleotide flipping step can be uncoupled from the bending of DNA in the formation of an ES complex.

In most organisms, the primary mechanism for the repair of ultraviolet (UV)[1] light-induced DNA photoproducts is the nucleotide excision repair pathway (NER) (*1*). However, in a modest subset of bacteria, and in some bacteriophage and viruses that infect eukaryotic cells, repair of the major UV photoproducts, the *cis-syn* cyclobutane pyrimidine dimers (CPD), can be initiated through the base excision repair (BER) pathway (reviewed in ref *2*). The initiation of BER at this dipyrimidine lesion is catalyzed by pyrimidine dimer glycosylases (Pdgs) (*3*). The most extensively characterized of these enzymes is the bacteriophage T4-Pdg. Pre- and postcatalytic events as measured by X-ray crystallography and fluorescence spectroscopy include flipping of the purine opposite the 5′-pyrimidine of the dimer into a cleft on the surface of the enzyme and bending of the DNA to a 60° angle (*4*, *5*). Once bound to a dimer site, T4-Pdg utilizes the α-NH_2 group of Thr2 and Glu23 to cleave the glycosyl bond of the 5′-dimer pyrimidine and the phosphodiester backbone via a β-elimination reaction (*6*−*10*).

The cocrystal structure of T4-Pdg with CPD-containing DNA was the first evidence of nucleotide flipping by a DNA repair enzyme (*5*), and recently, we have determined the cocrystal structure of T4-Pdg complexed as a reduced imine intermediate with abasic site-containing DNA (*11*). In the intervening time, the cocrystal structures of flipped and covalently bound complexes have been determined for several other DNA glycosylases, including uracil DNA glycosylases (UDGs) (*12*, *13*), 3-methyladenine DNA glycosylase (*14*, *15*), 8-oxoguanine DNA glycosylase (OGG1) (*16*, *17*), formamidopyrimidine DNA glycosylase (FPG) (*18*−*20*), and endonuclease VIII (*21*, *22*). A common property of these cocrystal complexes is the fact that specific amino acids occupy the "hole" in DNA that had been previously occupied by the extrahelical base. In the cases of T4-Pdg complexes, it was shown that the side chains of Arg22 and Arg26 partially fill the space previously occupied by the flipped nucleotide (*5*, *11*). In the covalently bound structure, the side chains of Arg22 and Arg26 were further embedded in the intrahelical volume created by nucleotide flipping in the enzyme−DNA complex. Conceptually similar proposals have been made for (1) *M.Hha*I using Gln237 as part of a push and bind mechanism (*23*), (2) *Escherichia coli* and human UDG using a Ser-Pro pinch and leucine residue as a hydrophobic wedge mechanism (*24*−*27*), and (3) *E. coli* MutY DNA glycosylase using Gly116 and Gly118, and Gly79 and Gly81, in a bend and pinch mechanism (*28*).

† This research was supported by National Institutes of Health Grants ES04091 and P30 ES06676.

* To whom correspondence should be addressed. Phone: (503) 494-9957. Fax: (503) 494-6831. E-mail: lloydst@ohsu.edu.

‡ PerkinElmer Life and Analytical Sciences.

§ Oregon Health and Science University.

[1] Abbreviations: BER, base excision repair; CPD, cyclobutane pyrimidine dimer; ES, enzyme−substrate; NER, nucleotide excision repair; Pdg, pyrimidine dimer glycosylase; OGG1, 8-oxoguanine DNA glycosylase; T4-Pdg, bacteriophage T4 pyrimidine dimer glycosylase; UDG, uracil DNA glycosylase; UV, ultraviolet; 2-AP, 2-aminopurine.

10.1021/bi060802s CCC: $33.50
Published on Web 11/04/2006

The biochemical and mechanistic studies of the catalytic mechanism of T4-Pdg have served as the paradigm for other glycosylase enzymes despite its unique feature of flipping the nucleotide opposite the lesion, rather than the damaged base itself. Our prior investigations of the precatalytic events in the T4-Pdg reaction utilized both noncleavable, high-affinity DNA substrates and catalytically inactive T4-Pdg mutants. Verdine and his colleagues have synthesized the former by designing transition-state analogues for DNA glycosylases (*29*, *30*). Using one of these substrates, a pyrrolidine-containing DNA, and other synthetic abasic sites (tetrahydrofuran or reduced AP site), we established that T4-Pdg binds with high affinity to these DNAs (*31*). These data provided the rationale for a fluorescence assay for monitoring nucleotide flipping. This was achieved by positioning a 2-AP opposite either the synthetic abasic site or CPD (*4*). Nucleotide flipping of the 2-AP resulted in a fluorescence enhancement as it moved from a quenched, stacked position within the DNA to the solvent-exposed surface of the protein. In addition, in contrast to what had been previously hypothesized, investigation of mutant T4-Pdg proteins demonstrated that specific binding does not require nucleotide flipping for complex stabilization; i.e., specific binding could be uncoupled from nucleotide flipping (*4*).

The exquisite selectivity of this assay was demonstrated by moving the 2-AP opposite the (nonscissile) 3′-base of the CPD in which no fluorescence enhancements were observed. These results suggest that in the case of T4-Pdg there is little general helical distortion that would give rise to the enhanced 2-AP fluorescence, and thus, its use as a measure of base flipping is well-justified. However, it should be noted that in some cases, the 2-AP-based fluorescence assay is not a clear indicator of base flipping in that, while some methyltransferases cause a significant enhancement of 2-AP fluorescence upon binding to a target site, others do not (*32*, *33*). Likewise, DNA distortions from events other than base flipping may lead to an enhanced 2-AP fluorescence (*34*).

The fluorescent properties of 2-AP have been used in analyzing the reaction mechanisms of a variety of other DNA reactive enzymes, including, but not limited to, UDG (*35*−*37*), photolyase (*38*−*40*), and, as indicated above, several methyltransferases (*32*, *41*−*43*). Collectively, these studies have revealed that these enzymes use a variety of mechanisms to achieve DNA bending and extrahelical movement of a nucleotide, ranging from a near-simultaneous expulsion of the base and DNA bending to temporally uncoupled precatalytic events. Since T4-Pdg is the only enzyme known to flip the nucleotide opposite the catalytic site and is known to severely kink DNA at the damaged site, we have developed an experimental strategy that allows analyses of nucleotide flipping and substrate duplex DNA bending by this protein. This design builds off our previous strategy using 2-AP as a fluorescent reporter combined with fluorescence resonance energy transfer. This investigation reveals a temporal uncoupling of the T4-Pdg-induced DNA bending and nucleotide flipping.

EXPERIMENTAL PROCEDURES

Materials. TAMRA-5-SE and QSY-7-SE were purchased from Molecular Probes (Eugene, OR). 5′-Amino modifier 5, dSpacer tetrahydrofuran, and 2-aminopurine CE phosphoramidites were purchased from Glen Research (Sterling, VA). 3-[(3-Cholamidopropyl)dimethylammonio]-1-propanesulfonate (CHAPS) was obtained from Boehringer Mannheim. Heparin grade I-A (porcine mucosa) was purchased from Sigma (St. Louis, MO).

Enzyme Expression and Purification. T4-Pdg was cloned, expressed, and purified as previously described (*44*). The purified enzyme was stored at 4 °C in 25 mM $NaHPO_4$ (pH 7.0), 25 mM NaCl, and 1 mM EDTA. Protein concentrations were determined from absorbance readings at 280 nm (minus 1.7 times the A_{320} reading to correct for any scatter), using a calculated molar extinction coefficient of 15 930 (*45*).

Oligonucleotide Synthesis. All oligonucleotides were synthesized in the Molecular Genetics Core facility (University of Texas Medical Branch, Galveston, TX) on a Perseptive Biosystems Expedite model 8909 instrument using 1 μmol 1000 A CPG columns. Crude synthates were purified by SPE on a Waters SepPak followed by RP (C18) HPLC with the product identity confirmed by MALDI-MS. Purified oligonucleotides were lyophilized and stored at −20 °C.

Oligonucleotide Labeling. Purified lyophilized 5′-amino-modified oligonucleotides were resuspended in 10 mM Tris-HCl (pH 8.0), 100 mM NaCl, and 0.1 mM EDTA (TEN buffer), and concentrations were determined by A_{260} measurements (1 OD = 50 μg/mL). A volume containing 100 μg of oligonucleotide was twice precipitated by the addition of 2.5 volumes of ethanol with 10 mM $MgCl_2$, centrifuged, and resupended in 85 μL of 0.2 M sodium borate (pH 8.5). The succinimidyl ester reactive dyes were dissolved in anhydrous acetonitrile, split into microfuge tubes in 250 μg aliquots, dried under vacuum in a SpeedVac, and stored at −20 °C. Oligonucleotide labeling was performed by redissolving 250 μg of the reactive dye in 15 μL of DMSO and mixing the sample with 100 μg of oligonucleotide in 85 μL of borate buffer. Reactions proceeded for ∼18 h at 22 °C, while the mixture was adjusted to 0.3 M NaCl and 10 mM $MgCl_2$ and twice precipitated with ethanol and the DNA resuspended in a final volume of 100 μL of TEN. The labeled DNAs were further purified through BioSpin 6 columns (Bio-Rad) that were previously equilibrated in TEN. Final purification was carried out by RP HPLC (250 mm × 4.6 mm Phenomenex Jupiter 300 A C4 column) using a linear gradient of 0.1 M triethylamine acetate (pH 7.0) to 60% acetonitrile developed over 60 min at 1 mL/min. The labeled oligonucleotide was collected, lyophilized, and stored at −20 °C.

Oligonucleotide Annealing. HPLC-purified oligonucleotides were resuspended in TEN, and concentrations were estimated by A_{260} measurements. A typical annealing reaction mixture consisted of the TAMRA-labeled oligonucleotide strand mixed with a 1.1-fold molar excess of the unlabeled strand or QSY-labeled strand, was heated to 90 °C, and was allowed to cool slowly to 4 °C using a PCR instrument. Duplex oligonucleotides were isolated from single-stranded DNA by anion exchange HPLC (250 mm × 4.6 mm SynchroPak AX 300 column), using a linear gradient from 10 mM potassium phosphate (pH 7.0) and 0.1 mM EDTA (buffer A) to 2 M KCl in buffer A over 60 min at a rate of 1 mL/min. The duplex-containing peak was collected and concentrated in a Centricon YM-3 filter (Amicon) and exchanged into TEN buffer using the same centrifugation filtration device.

Fluorescence Measurements. All fluorescence measurements were performed on a SPEX (Edison, NJ) Fluorolog-2 spectrofluorometer with data acquisition in the photon counting mode and with sample temperatures maintained at 25 °C by a circulating water bath.

Emission Spectra. Ratiometric spectra were collected at 1 nm intervals with a 1 s integration per step. Sample spectra were collected in 220 μL of PKC buffer (containing 10 mM potassium phosphate, 100 mM KCl, and 0.1% CHAPS) on DNA alone, DNA with 1 μM T4-Pdg, and DNA with 1 μM T4-Pdg and 4 mg/mL heparin. Spectra for T4-Pdg and or heparin were collected and used for background subtraction corrections. Measurements for 2-AP-containing oligonucleotides were taken using a sample concentration of 80 nM with the excitation at 315 nm (3.5 nm bandpass) and emission passed through a KV 370 filter (Schott) and into an emission monochromator scanned from 330 to 450 nm (15 nm bandpass). Measurements for TAMRA-5 were obtained using 80 nM DNA with excitation at 540 nm (1.77 nm bandpass) and emission passed through an OG 570 long-pass filter (Schott) and into an emission monochromator scanned from 550 to 620 nm (5 nm bandpass).

Fluorescence Equilibrium Titrations. Equilibrium titrations were carried out in PKC buffer by using starting oligonucleotide concentrations of 10, 20, or 30 nM and adding microliter aliquots of T4-Pdg. Volume changes did not exceed 5%, and titrations were corrected for dilution effects and background contributions of enzyme-only controls. Mixtures were allowed to equilibrate for 1.5 min before the fluorescence intensity was recorded. Measurements of the magnitude of the 2-AP signal were carried out in a 1.1 mL reaction volume with excitation at 315 nm (3.5 nm bandpass), and emission was recorded at 380 nm (15 nm bandpass) using a KV-370 long-pass filter. Measurements of the magnitude of the TAMRA signal were carried out in a 220 μL reaction volume with excitation at 550 nm (1.77 nm bandpass) and emission recorded at 585 nm (5 nm bandpass) using an OG-570 long-pass filter (Schott). The K_d(app) for binding was determined from simultaneous fits of data from three DNA concentrations as described in the data analyses.

Fluorescence Stopped-Flow Experiments. Stopped-flow measurements were performed using an OLIS-USA-SF (OLIS, Jefferson, GA) flowbox that was attached to a SPEX fluorolog-2 fluorometer. The instrument dead time was determined to be 3 ms. Due to either low signal intensities or small amplitude changes involved in the measurements, it was necessary to average six to eight successive shots for each experimental determination. Data were recorded in 2 ms intervals using a 2 ms signal integration. Measurements involving the 2-AP signal were performed using a λ_{ex} of 315 nm (3.5 nm bandpass) and a λ_{em} of 380 nm (15 nm bandpass) using a KV-370 emission filter (Schott). Measurements of the magnitude of the TAMRA signal were performed using a λ_{ex} of 550 nm (1.5 nm bandpass) and a λ_{em} of 585 nm (5 nm bandpass) using an OG-570 emission filter (Schott). Determinations of association rates were made by rapidly mixing an equal volume of enzyme solution (200−700 nM) with DNA (80 nM). Determinations of dissociation rates were performed by rapidly mixing preformed ES complex (100 nM T4-Pdg and 80 nM DNA) with an equal volume of heparin (8 mg/mL).

Calculation of Equilibrium Binding Constants. Titrations were performed by adding enzyme to fixed DNA concentrations that were near the K_d value. The data were analyzed assuming a simple binding model, and data sets consisting of 10, 20, and 30 nM DNA were simultaneously fit by nonlinear regression to eq 1:

$$F_{obs} = F_o + \left(\frac{F_{max} - F_o}{2D_t}\right)[E_t + D_t + K_d - \sqrt{(E_t + D_t + K_d)^2 - 4E_tD_t}] \quad (1)$$

where F_{obs} is the measured magnitude of the signal, F_o is the fitted initial fluorescence intensity, F_{max} is the magnitude of the fitted limiting fluorescence signal at saturating enzyme levels, E_t is the known total added enzyme concentration, D_t is the known fixed DNA concentration, and K_d is the fitted dissociation equilibrium constant.

Calculation of Association Rate Constants. Stopped-flow experiments were performed under assumed pseudo-first-order conditions, and traces were fit by nonlinear regression analysis to a single-exponential rise according to eq 2:

$$F_{obs} = \text{offset} + \text{amp}(1 - e^{-k_{obs}t}) \quad (2)$$

in which F_{obs} is the magnitude of the signal measured as a function of time, offset is the magnitude of the fitted signal at time zero, amp is the fitted amplitude, and k_{obs} is the observed rate constant. Extracted observed rate constants were plotted against their corresponding enzyme concentrations, and the bimolecular rate constant was determined from the slope of the line calculated from linear regression analysis.

Calculation of Dissociation Rate Constants. Stopped-flow experiments were modeled as unimolecular processes due to the irreversibility conferred by the heparin trap. Data derived from TAMRA experiments were fit to a single-exponential rise according to eq 2, and 2-AP data were fit to eq 3

$$F_{obs} = \text{offset} + \text{amp} \times e^{-k_{obs}t} \quad (3)$$

where F_{obs} is magnitude of the the signal measured as a function of time, offset is the magnitude of the fitted signal at time zero, amp is the fitted amplitude, and k_{obs} is the observed rate constant. Fits were performed by nonlinear least-squares regression using KinFit (OLIS).

RESULTS

Characterization of the 2-AP Flipping Signal in Duplex DNA Opposite Tetrahydrofuran. Using a 21-mer duplex DNA in which a centrally located 2-AP in one strand was positioned opposite an abasic site analogue, tetrahydrofuran [designated ds(2AP−TF) (Table 1)], the utility of 2-AP as a nucleotide flipping signal was demonstrated by the emission spectra in the absence or presence of T4-Pdg. The excitation wavelength was set at 315 nm to isolate the 2-AP signal from any contribution from tryptophan fluorescence provided by T4-Pdg. As shown in Figure 1, the fluorescence intensity of 2-AP in ds(2AP−TF) increased 2.8-fold when a saturating concentration of T4-Pdg was added, a result that is in excellent agreement with data previously reported (*4*). The

Table 1: Duplex Oligonucleotide Substrates[a]

ds(2AP/TF)	GTTCCAGCTA2GCTCAGGTTC CAAGGTCGATdCGAGTCCAAG
ds(TAM-2AP/TF)	TAM-GTTCCAGCTA2GCTCAGGTTC CAAGGTCGATdCGAGTCCAAG
ds(TAM-2AP/QSY-TF)	TAM-GTTCCAGCTA2GCTCAGGTTC CAAGGTCGATdCGAGTCCAAG-QSY

[a] In the 5′ → 3′ direction (top strand). TAM stands for TAMRA, QSY for QSY-7, d for tetrahydrofuran, and 2 for 2-aminopurine.

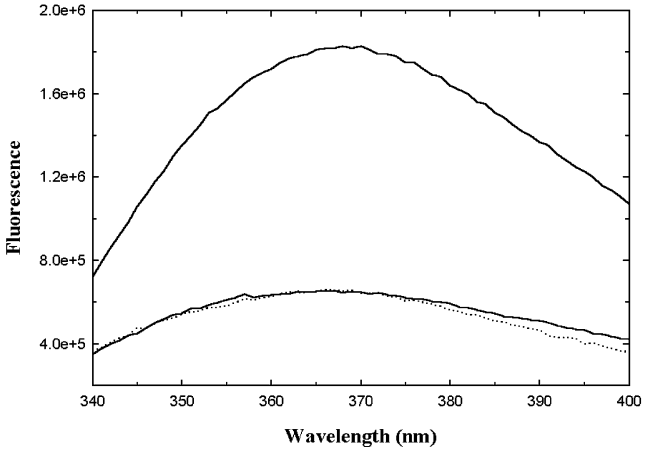

FIGURE 1: Fluorescence spectra of ds(2AP−TF) in the presence or absence of T4-Pdg. Measurements were taken in 10 mM KH_2PO_4, 100 mM KCl, and 0.1% CHAPS at pH 6.8 and 25 °C. The following samples were used: 80 nM ds(2AP−TF) (bottom solid line), 80 nM ds(2AP−TF) with 1 μM T4-Pdg (top solid line), and ds(2AP−TF) with 1 μM T4-Pdg and 4 mg/mL heparin (dotted line). Spectra were recorded using a λ_{ex} of 315 nm and a λ_{em} of 380 nm.

enhanced signal could be reversed by the addition of excess heparin, thus demonstrating that the enhanced fluorescence signal was due to reversible binding by the enzyme. The use of heparin to compete for DNA binding enzymes has been previously described (*46*).

Equilibrium Measurements of Binding of T4-Pdg to ds(2AP−TF). The increase in the intensity of 2-AP in ds(2AP−TF) upon binding by T4-Pdg provided a convenient signal for detecting formation of the enzyme−DNA complex. Equilibrium experiments were performed by titrating ds(2AP−TF) with T4-Pdg and using the change in the magnitude of the 2-AP signal as a measure of binding. Due to the relatively weak fluorescence provided by 2-AP, it was necessary to use relatively high concentrations of the duplex DNA to acquire reliable signals. Experimental data sets consisted of three separate titrations at different DNA concentrations that were near the K_d. Global fitting of the data sets to a quadratic binding equation was performed as described in the data analysis. Figure 2 shows a representative data set that demonstrated that the magnitude of the signal increased monotonically and was saturable with increasing concentrations of T4-Pdg. Multiple data sets were analyzed with a resulting mean K_d of 28.4 ± 3.3 nM (Table 2).

Stopped-Flow Measurements of T4-Pdg Binding. To gain further insight into the nature of the change in the magnitude of the 2-AP signal as modulated by the addition of T4-Pdg, pre-steady-state measurements were made using a fluorescence stopped-flow methodology. Experiments were designed to follow the association or dissociation of the enzyme−substrate complexes, using the change in the magnitude of the 2-AP signal as a reporter for the interaction. The association rates were measured under pseudo-first-order conditions by adding excess concentrations of T4-Pdg relative to ds(2AP−TF) and monitoring the increase in the magnitude of the 2-AP fluorescence signal. Traces from four to nine replicate shots for each T4-Pdg concentration were averaged to improve the signal-to-noise ratio and were fitted to a single-exponential rise to determine a pseudo-first-order rate constant. As shown in Figure 3, there was a linear increase in the observed rate constants with increasing concentrations of substrate with an intrinsic association rate constant (k_{on}) of 9.78 × 10^8 M^{-1} s^{-1} calculated by linear regression analysis.

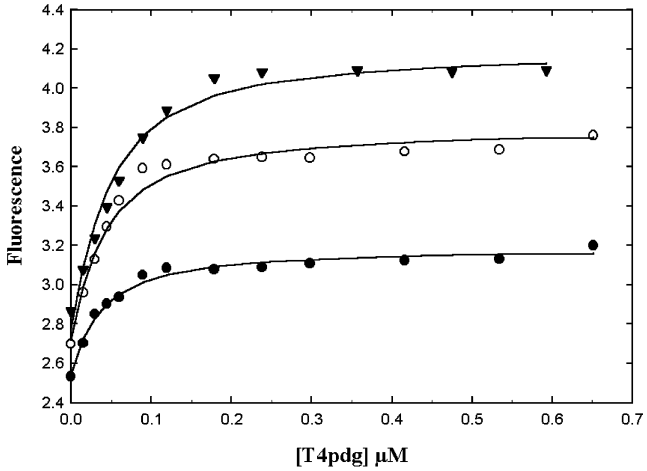

FIGURE 2: Equilibrium binding measurements of T4-Pdg and ds(2AP−TF). Titrations were performed in PKC buffer using three fixed concentrations of ds(2AP−TF): 10 (●), 20 (○), and 30 nM (▼). The lines drawn are from a global fit of the data described in the data analysis. Shown is a representative data set with a K_d of 24.9 ± 10.2 nM.

The dissociation of the ES complex was assessed by mixing preformed enzyme−DNA complexes with 8 mg/mL heparin and monitoring the decrease in the magnitude of the 2-AP signal (Figure 4). Traces from five to eight replicate shots were averaged and fitted to a single-exponential decrease. These data were adequately described by a single exponential, and the quality of the fits was not statistically improved when data were fit to higher-order exponentials. Control experiments in which the heparin concentration was increased to 16 mg/mL did not change the results of the fits, indicating that the rate of binding of heparin to the free enzyme was sufficiently greater than the rate of rebinding of the enzyme to the DNA substrate (data not shown). The results were reproducible with a high degree of precision, with the average of four data sets resulting in a dissociation rate constant (k_{off}) of 24 s^{-1} (Table 2). The K_d, as calculated from the k_{off}/k_{on} ratio, was 25.6 nM and is in excellent agreement with the K_d of 28.4 nM determined from equilibrium binding studies. This convergence of the equilibrium and pre-equilibrium results supports the validity of using the 2-AP signal for monitoring the enzyme−substrate interaction.

Characterization of the 2-AP Fluorescence. To concomitantly assess nucleotide flipping and DNA bending, it was necessary to modify the ds(2AP−TF) duplex substrate by adding fluorescent donor and acceptor molecules to the two

Table 2: Summary of Kinetic and Equilibrium Constants Derived for T4-Pdg with ds(2AP−TF) and ds(TAM-2AP−QSY-TF) Substrates

substrate	K_d (nM)[a]	K_d (nM)[b]	k_{on} (M^{-1} s^{-1})[a]	k_{off} (s^{-1})[a,c]	$k_{off\,(S}$ $^{-1})$[b,c]
ds(2AP−TF)	28.4 ± 3.3[d]	nd[e]	(9.78 ± 0.2) × 10^8	24 ± 2.5[f]	nd[e]
ds(TAM-2AP−QSY-TF)	21.4 ± 4.2[d]	26.7 ± 6.3[d]	nd[e]	25 ± 1[f]	62 ± 5[g]

[a] Estimated from 2-AP fluoresence. [b] Estimated from FRET analyses. [c] Six to nine replicate shots were collected and averaged per stopped-flow experiment. [d] Mean ± the standard deviation (SD) (n = 3). [e] Not detemined. [f] Mean ± SD (n = 4). [g] Mean ± SD (n = 5).

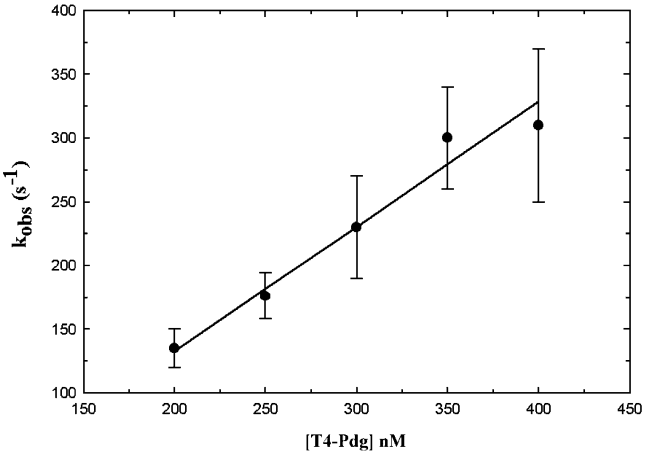

FIGURE 3: Association rate constant for T4-Pdg and ds(2AP−TF). Pseudo-first-order rate constants for the association of ds(2AP−TF) with T4-Pdg were determined by fluorescence stopped-flow experiments in PKC buffer using 80 nM ds(2AP−TF) (syringe A) and increasing concentrations of T4-Pdg (syringe B). The values were derived from four to nine replicate traces and are plotted with error bars corresponding to the 95% confidence limits. The line is from a weighted linear regression analysis using the relative errors in the k_{obs} values to obtain an intrinsic association rate constant of (9.78 ± 0.2) × 10^8 M^{-1} s^{-1}.

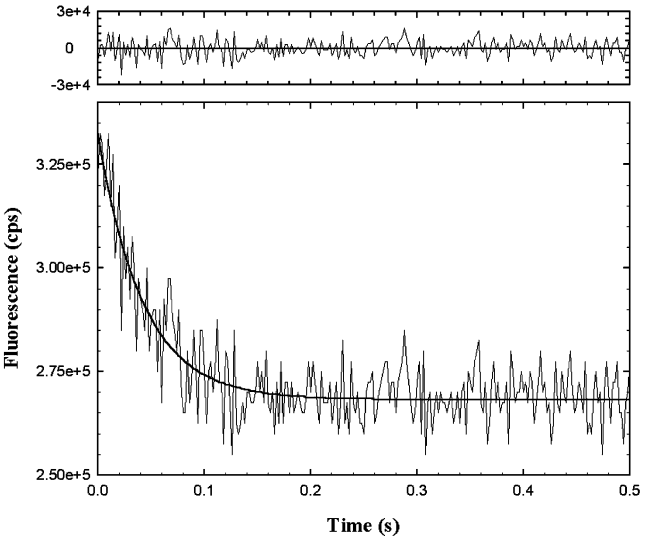

FIGURE 4: Dissociation rate constant for T4-Pdg and ds(2AP−TF). Dissociation rate constants were determined by fluorescence stopped-flow measurements. Experiments were performed in PKC buffer by mixing 80 and nM T4-Pdg (syringe A) with 8 mg/mL heparin (syringe B). Data were recorded in 2 ms steps with a λ_{ex} of 315 nm and a λ_{em} of 380. Between five and eight traces were averaged and fit to a single exponential as described in the data analysis. Shown is a representative data set with a k_{off} of 23.6 ± 1.4 s^{-1}. The residuals to the fitted line are shown in the top panel.

strands. Thus, this new substrate [termed ds(TAM-2AP−QSY-TF)] (Table 1) was designed with an internal 2-AP−tetrahydrofuran pair for assessing nucleotide flipping, as described above, and an end labeled TAMRA−QSY-7 pair for assessing DNA bending (Table 1). However, prior to those investigations, it was necessary to assess whether the TAMRA−QSY-7 pair had any affect on the 2-AP emission profile. Emission spectra of this new substrate, ds(TAM-2AP−QSY-TF), were recorded in the absence or presence of T4-Pdg (Figure 5a). The 2-AP spectra of the two duplex DNAs were indistinguishable, with comparable 2.8-fold increases in intensities in the presence of saturating T4-Pdg levels. This enhancement could be fully reversed by the addition of heparin. These data indicate that the addition of TAMRA and QSY-7 dyes did not interfere with the flipping of the 2-AP.

Characterization of the TAMRA Fluorescence. The TAMRA and QSY-7 dyes have spectral overlap and form a donor−receptor energy transfer pair. The ds(TAM-2AP−QSY-TF) substrate was designed with this pair on opposite ends of a duplex oligonucleotide so that any change in the distance of the ends would result in a change in TAMRA intensity. Since previous structural studies had shown that T4-Pdg binding resulted in an ∼60−66° kink in the DNA (*5*, *11*), experiments were carried out on this duplex to investigate whether DNA bending could be detected spectroscopically using the TAMRA−QSY-7 energy transfer pair. The emission spectrum of the TAMRA-derived signal of the duplex DNA is shown in Figure 5b. A 15% decrease in fluorescence intensity was observed when T4-Pdg was added. This fluorescence was interpreted as a decrease due to the decreased distance between the dyes as a result of the bent DNA complex. The change in signal was due to reversible binding by T4-Pdg as evidenced by the fluorescent signal being restored to the original level using a heparin trap methodology. Importantly, the fluorescence change was dependent upon the presence of acceptor QSY-7. This is clearly demonstrated and shown in Figure 5c, in which there was no effect on TAMRA fluorescence in the singly labeled duplex substrate DNA, in which the complementary strand was not labeled with QSY-7. These results are consistent with fluorescence quenching arising from the increased efficiency of energy transfer arising from the proximity of the ends of the DNA as a consequence of a bend caused by T4-Pdg binding.

Equilibrium Measurements of Binding of T4-Pdg to ds(TAM-2AP−QSY-TF). To further characterize ds(TAM-2AP−QSY-TF), equilibrium binding experiments were performed by titrating the substrate with T4-Pdg and measuring either the 2-AP- or TAMRA−QSY-7-derived signals. Titrations were performed at three concentrations of duplex DNA and analyzed as described in Experimental Procedures. Representative data sets are shown in panels a and b of Figure 6, and the results are summarized in Table 2. The K_ds obtained by measuring 2-AP and TAMRA signals were 21.4 ± 4.2 and 26.7 ± 6.3 nM, respectively. The statistical equivalence of these two measurements suggests that the two

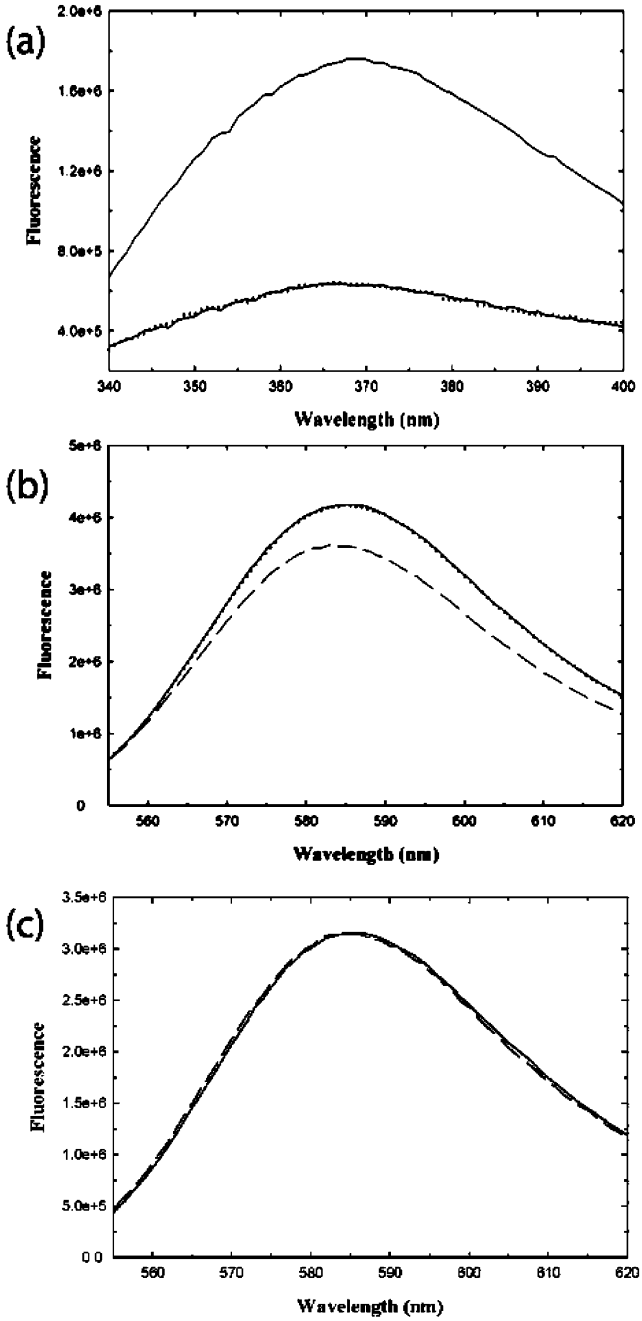

FIGURE 5: Fluorescence spectra of ds(TAM-2AP−QSY-TF) and ds(TAM-2AP−TF) in the presence or absence of T4-Pdg. Measurements were taken in PKC buffer at 25 °C. (a) The following 2-AP fluorescence samples were used: 80 nM ds(TAM-2AP−QSY-TF) (bottom solid line), 80 nM ds(TAM-2AP−QSY-TF) with 1 μM T4-Pdg (top solid line), and ds(TAM-2AP−QSY-TF) with 1 μM T4-Pdg and 4 mg/mL heparin (dotted line). Spectra were recorded using a λ_{ex} of 315 nm and a λ_{em} of 380 nm. (b) The following TAMRA fluorescence samples were used: 80 nM ds(TAM-2AP−QSY-TF) (solid line), 80 nM ds(TAM-2AP−QSY-TF) with 1 μM T4-Pdg (dashed line), and ds(TAM-2AP−QSY-TF) with 1 μM T4-Pdg and 4 mg/mL heparin (dotted line). Spectra were recorded using a λ_{ex} of 550 nm and a λ_{em} of 585 nm. (c) The following TAMRA fluorescence samples that were dependent on QSY-7 were used: 80 nM ds(TAM-2AP−TF) (solid line) and 80 nM ds(TAM-2AP−TF) with 1 μM T4-Pdg (dashed line). Spectra were recorded using a λ_{ex} of 550 nm and a λ_{em} of 585 nm.

signals may be reporting on the same end point (i.e., the ES complex that is both flipped and bent).

Stopped-Flow Analyses. Although the equilibrium measurements using the 2-AP or TAMRA signal appear to be

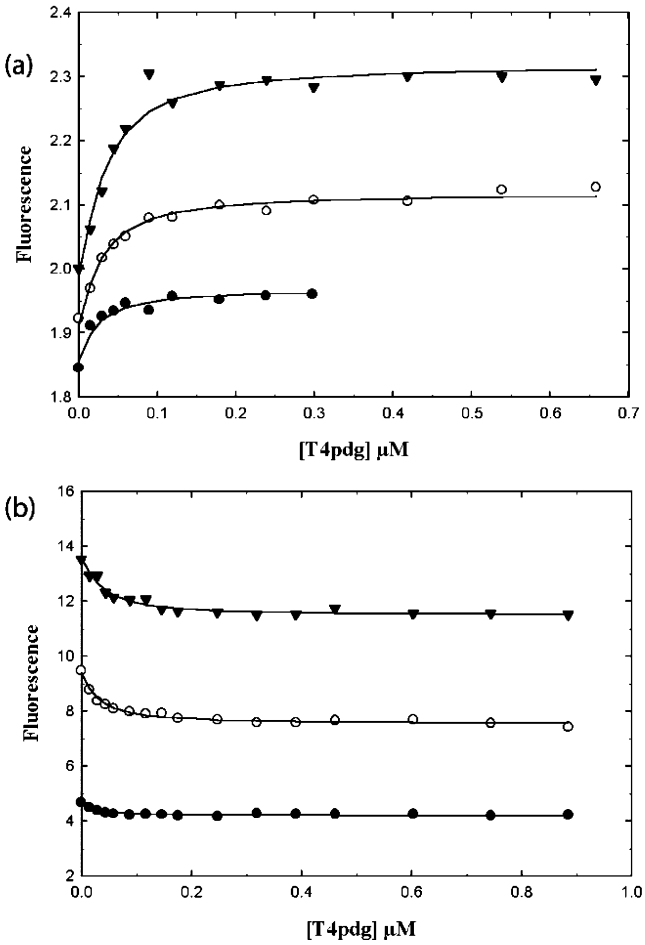

FIGURE 6: Equilibrium binding measurements of T4-Pdg with ds(TAM-2AP−QSY-TF). Titrations were performed in PKC buffer at three fixed concentrations of ds(TAM-2AP−QSY-TF): 10 (●), 20 (○), and 30 nM (▼). The lines drawn are from a global fit of the data as described in the data analysis. (a) The 2-AP fluorescence is a representative data set using a λ_{ex} of 315 nm and a λ_{em} of 380 nm with a K_d of 19 ± 6.1 nM. (b) The TAMRA fluorescence is a representative data set using a λ_{ex} of 550 nm and a λ_{em} of 585 nm with a K_d of 21.4 ± 5.3 nM.

equivalent, a pre-steady-state kinetic study was undertaken to explore possible differences in the time-dependent changes in either signal. Stopped-flow experiments were performed by mixing a solution of preformed T4-Pdg−ds (TAM-2AP−QSY-TF) complexes with heparin and monitoring either the signal derived from 2-AP (flipping) or the TAMRA (bending) fluorescence. Due to the relatively small changes in amplitude in the TAMRA signal and fast rates that were encountered, it was not possible to obtain reliable association rates. Also, due to the low signal-to-noise ratios, between six and nine consecutive shots were averaged prior to fitting analyses. Experiments measuring the 2-AP signal in this duplex (Figure 7a) were fit to a single-exponential decrease, with a calculated average rate constant of 25 ± 1 s^{-1} (Table 2). These results were statistically indistinguishable from that obtained with ds(2AP−TF), indicating that the double-end labeling did not fundamentally alter the substrate from a mechanistic point of view. Interestingly, stopped-flow experiments that monitored the TAMRA−QSY-7 signal under conditions that were identical to those for the 2-AP measurements resulted in dissociation rates that were significantly faster (Figure 7b). The traces from the TAMRA−QSY-7 data sets were adequately described by a single-exponential rise

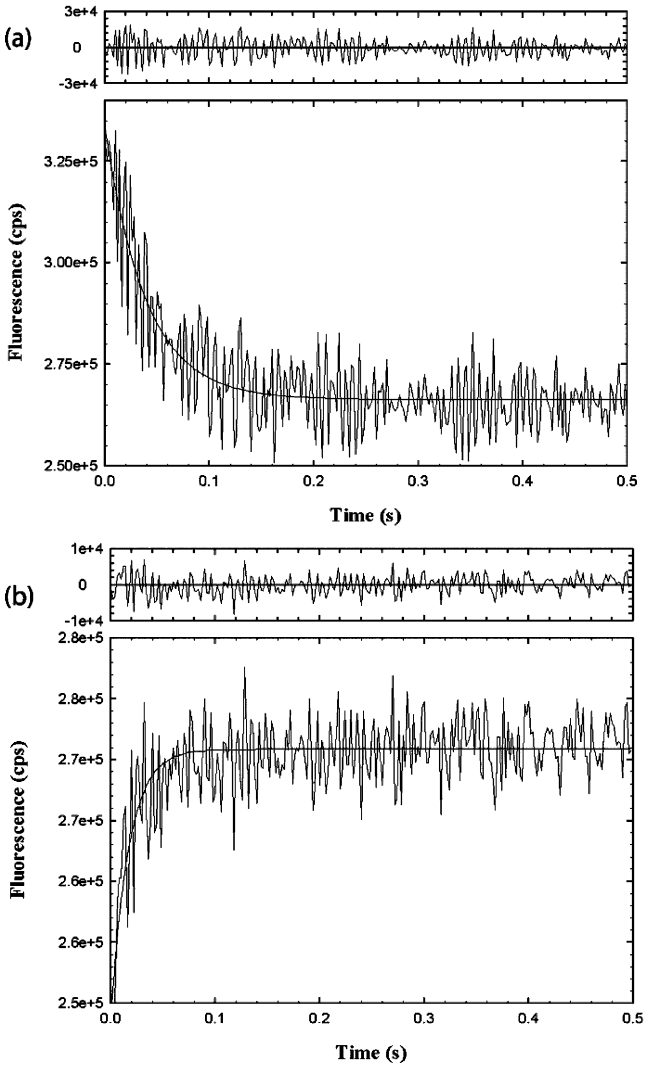

FIGURE 7: Dissociation of the ds(TAM-2AP−QSY-TF)−T4-Pdg complex following the 2-AP nucleotide flipping signal and the TAMRA DNA bending signal. Dissociation rate constants were determined by fluorescence stopped-flow measurements. Experiments were performed in PKC buffer by mixing 80 and 200 nM T4-Pdg (syringe A) with 8 mg/mL heparin (syringe B). (a) For the 2-AP nucleotide flipping signal, data were recorded in 2 ms steps with a λ_{ex} of 315 nm and a λ_{em} of 380. Between six and nine traces were averaged and fit to a single-exponential fall as described in the data analysis. Shown is a representative data set with a k_{off} of 24.1 ± 1.2 s^{-1}. The residuals to the fitted line are shown in the top panel. (b) For the TAMRA DNA bending signal, data were recorded in 2 ms steps with a λ_{ex} of 550 nm and a λ_{em} of 585. Between six and nine traces were averaged and fit to a single-exponential rise as described in the data analysis. Shown is a representative data set with a k_{off} of 59 ± 7 s^{-1}. The residuals to the fitted line are shown in the top panel.

and were not improved when fit to higher-order exponential processes. Analyses of these data resulted in an average dissociation rate constant of 62 ± 5 s^{-1} (Table 2). Additionally, there was no discernible lag corresponding to the time constant for the nucleotide flipping process.

DISCUSSION

The binding of T4-Pdg to a *cis-syn* cyclobutane pyrimidine dimer-containing DNA substrate is characterized by the formation of an ES complex in which the adenine opposite the 5′-T of the lesion is moved to an extrahelical position in a binding pocket on the enzyme with a 60−66° kink introduced into the DNA backbone at the site of the lesion. These flipped and bent structures were evident in both cocrystal structures that have been determined for T4-Pdg (*5*, *11*) and provide valuable information and insight into the mechanism of T4-Pdg. However, these structures provide only static pictures of the mechanistic processes. To provide a dynamic picture of the precatalytic events, we used oligonucleotide substrates containing strategically positioned fluorescent reporter groups. The placement of 2-AP opposite the binding site allowed measurements of nucleotide flipping, while end labeling with a donor−quencher pair allowed measurements of the degree of DNA bending. The use of the abasic site analogues as models for pyrimidine dimers is well-justified since comparative analyses of the two cocrystal structures revealed only modest changes in the positioning of the extrahelical nucleotide, with most differences being in the position of specific side chains associated with the stabilization of the flipped nucleotide. Pre-steady-state and equilibrium analyses of interactions of T4-Pdg with these substrates provide evidence that nucleotide flipping and DNA bending occur on different time scales. This conclusion is reached from the analysis of the dissociation rates of the saturated enzyme−DNA complex in which reversal of the DNA bending signal was 2.5-fold greater in magnitude than that observed for relaxation of base flipping. The implications of these results are that base flipping and DNA bending are temporally separated on the pathway leading to the formation of the Michaelis complex. The possibility that the two events are random or can occur independent of one another is unlikely. To prevent the violation of the law of microscopic reversibility, two separate enzyme−substrate binding modes would need to be invoked. However, the near equivalence of the K_ds measured for flipping and bending suggests similar binding interactions, presumably from the same binary complex. These conclusions are further supported by the similarity in the structures of the noncovalent and covalent crystal structures. On the basis of the correlation of the fluorescence data with the structural data, the interpretation of the enhanced fluorescence as a measure of base flipping is well-justified. However, it should be noted that in the absence of analyses such as time-resolved fluorescence (*47*), we cannot rule out definitively the possibility of other non-base-flipping distortions giving rise to the enhanced fluorescence.

Additionally, the footprint of T4-Pdg is estimated to be 11 bases, which argues against multiple enzyme molecules binding to the same oligonucleotide substrate (*48*). Therefore, the flipping and bending signals are measuring different intermediates in dissociation of a common complex, and the 2.5-fold difference in off rates for flipping and bending indicates that flipping and bending are not simultaneous events.

The apparent association rate constant derived from the concentration-dependent linear increase in the observed k_{on} measured from 2-AP fluorescence was near the diffusion limit at 9.8×10^8 M^{-1} s^{-1}. Using equilibrium and pre-steady-state measurements monitoring 2-AP fluorescence, an estimate of the association rate constant, calculated as k_{off}/K_d, was 8×10^8 M^{-1} s^{-1}. The convergence of these results is consistent with an equilibrium between the free enzyme and substrate and the flipped nucleotide complex, suggesting that the base flipping measurement is also indicative of the

enzyme−DNA binding event. Additionally, in the course of identifying substrates that would be appropriate for this study, we prepared an oligonucleotide in which the 5′-end was labeled with the fluorophore Alexa 488. The fluorescence intensity of this substrate was significantly quenched in the presence of T4-Pdg (data not shown). Stopped-flow measurements of the rate of quenching of this substrate by T4-Pdg resulted in an estimation of an apparent association rate constant of approximately 9×10^8 M^{-1} s^{-1}. The comparable magnitude of this measurement and that of the 2-AP substrate may suggest that the enzyme−DNA interaction is near the diffusion limit and, thus, nucleotide flipping is either concomitant with DNA binding or occurs in a fast step following the initial encounter. These data are similar to the results obtained for the *M.Eco*RI DNA methyltransferase, where the processes of DNA binding and base flipping were observed to be nearly simultaneous (*32*).

The association rate following the bending signal could not be directly measured due to signal noise relative to amplitude changes. However, an apparent association rate constant, calculated as the k_{off}/K_d ratio, was approximately 2.5×10^9 M^{-1} s^{-1}, which is significantly greater than that determined from the flipping data or quenching experiments. Therefore, the sequential ordering of the two processes in light of these considerations leads to our proposal of a reaction pathway for T4-Pdg in which nucleotide flipping precedes DNA bending. In this interpretation, the binding of the enzyme to DNA results in the extrahelical movement of the base opposite the lesion into the binding cleft on the enzyme. This encounter is followed by a putative conformational change in which the DNA is bent. Presumably, this is the structure necessary for the formation of a Michaelis complex.

Comparisons of this proposal with data derived from the analyses of other enzymes that carry out nucleotide flipping mechanisms reveal diversity in the sequential order of DNA bending and flipping. In the case of UDG, the Stivers group has demonstrated that among the earliest stages of the flipping reaction, UDG stabilizes an open state of the duplex without increasing the rate constant for spontaneous base pair opening (*49*). They conclude that examination of an extrahelical T of an A-T base pair occurs through a process in which the prebound enzyme transiently traps the extrahelical base without inducing a DNA bend. Concomitant studies from the Stivers group revealed that subsequent enzyme-induced DNA bending promotes the forward steps toward a fully flipped state as evidenced by loss of base stacking interactions and the removal of hydrogen bonding (*50*, *51*). Data presented in this study do not reveal evidence that supports or refutes a similar partial flipping model for T4-Pdg. It is also possible that there is an initial partial bend that is not kinetically observable due to exceptionally fast rates.

In contrast to these UDG data, the Verdine group presented evidence that OGG1 binds and bends nonspecific and lesion-specific containing DNAs to similar extents (*16*). They have also demonstrated by cocrystallization of OGG1 and normal DNA that OGG1 samples normal G nucleobases in an extrahelical position that was intermediate to insertion into the enzyme active site (*17*). More recently, the Verdine group has demonstrated that in the process of searching for DNA lesions, MutM inserts the side chain of Phe114 into duplex DNA, buckling base pairs that remain intrahelical while severely bending the DNA (*52*).

The kinetics of DNA binding, bending, and nucleotide flipping have also been measured for DNA methyltransferases. Hopkins and Reich (*42*) used FRET analyses to determine that despite the observed bending of the cognate sequence, the binding of the *E. coli* adenine methyltransferase (*M.Eco*RI) to substrate DNA resulted in a decreased level of energy transfer between several combinations of donor−acceptor pairs. This was explained as an expansion of the helix due to intercalation by the enzyme. DNA binding, base flipping, and DNA bending for *M.Eco*RI have been shown to be simultaneous events (*42*).

Collectively, these studies reveal a two- or three-step (depending on the enzyme) recognition process (specific binding, flipping, and bending) that allows several levels of regulation to help ensure proper substrate recognition before a catalytically competent ES complex is formed. Parameters that would interfere with either DNA bending or nucleotide flipping would result in an abortive encounter allowing for higher specificity.

ACKNOWLEDGMENT

We thank Ritche Jabil for technical assistance and Dr. M. L. Dodson for insightful discussions.

REFERENCES

1. Sancar, A., Lindsey-Boltz, L. A., Unsal-Kacmaz, K., and Linn, S. (2004) Molecular mechanisms of mammalian DNA repair and the DNA damage checkpoints, *Annu. Rev. Biochem. 73*, 39−85.
2. Huffman, J. L., Sundheim, O., and Tainer, J. A. (2005) DNA base damage recognition and removal: New twists and grooves, *Mutat. Res. 577*, 55−76.
3. Lloyd, R. S. (2005) Investigations of pyrimidine dimer glycosylases: A paradigm for DNA base excision repair enzymology, *Mutat. Res. 577*, 77−91.
4. McCullough, A. K., Dodson, M. L., Scharer, O. D., and Lloyd, R. S. (1997) The role of base flipping in damage recognition and catalysis by T4 endonuclease V, *J. Biol. Chem. 272*, 27210−7.
5. Vassylyev, D. G., Kashiwagi, T., Mikami, Y., Ariyoshi, M., Iwai, S., Ohtsuka, E., and Morikawa, K. (1995) Atomic model of a pyrimidine dimer excision repair enzyme complexed with a DNA substrate: Structural basis for damaged DNA recognition, *Cell 83*, 773−82.
6. Schrock, R. D. d., and Lloyd, R. S. (1991) Reductive methylation of the amino terminus of endonuclease V eradicates catalytic activities. Evidence for an essential role of the amino terminus in the chemical mechanisms of catalysis, *J. Biol. Chem. 266*, 17631−9.
7. Schrock, R. D. d., and Lloyd, R. S. (1993) Site-directed mutagenesis of the NH_2 terminus of T4 endonuclease V. The position of the α NH_2 moiety affects catalytic activity, *J. Biol. Chem. 268*, 880−6.
8. Manuel, R. C., Latham, K. A., Dodson, M. L., and Lloyd, R. S. (1995) Involvement of glutamic acid 23 in the catalytic mechanism of T4 endonuclease V, *J. Biol. Chem. 270*, 2652−61.
9. Dodson, M. L., Schrock, R. D. d., and Lloyd, R. S. (1993) Evidence for an imino intermediate in the T4 endonuclease V reaction, *Biochemistry 32*, 8284−90.
10. Doi, T., Recktenwald, A., Karaki, Y., Kikuchi, M., Morikawa, K., Ikehara, M., Inaoka, T., Hori, N., and Ohtsuka, E. (1992) Role of the basic amino acid cluster and Glu-23 in pyrimidine dimer glycosylase activity of T4 endonuclease V, *Proc. Natl. Acad. Sci. U.S.A. 89*, 9420−4.
11. Golan, G., Zharkov, D. O., Grollman, A. P., Dodson, M. L., McCullough, A. K., Lloyd, R. S., and Shoham, G. (2006) Structure of T4 Pyrimidine Dimer Glycosylase in a Reduced Imine Covalent Complex with Abasic Site-containing DNA, *J. Mol. Biol. 362*, 241−58.

12. Slupphaug, G., Mol, C. D., Kavli, B., Arvai, A. S., Krokan, H. E., and Tainer, J. A. (1996) A nucleotide-flipping mechanism from the structure of human uracil-DNA glycosylase bound to DNA, *Nature 384*, 87−92.
13. Barrett, T. E., Savva, R., Panayotou, G., Barlow, T., Brown, T., Jiricny, J., and Pearl, L. H. (1998) Crystal structure of a G:T/U mismatch-specific DNA glycosylase: Mismatch recognition by complementary-strand interactions, *Cell 92*, 117−29.
14. Lau, A. Y., Scharer, O. D., Samson, L., Verdine, G. L., and Ellenberger, T. (1998) Crystal structure of a human alkylbase-DNA repair enzyme complexed to DNA: Mechanisms for nucleotide flipping and base excision, *Cell 95*, 249−58.
15. Hollis, T., Lau, A., and Ellenberger, T. (2000) Structural studies of human alkyladenine glycosylase and *E. coli* 3-methyladenine glycosylase, *Mutat. Res. 460*, 201−10.
16. Chen, L., Haushalter, K. A., Lieber, C. M., and Verdine, G. L. (2002) Direct visualization of a DNA glycosylase searching for damage, *Chem. Biol. 9*, 345−50.
17. Banerjee, A., Yang, W., Karplus, M., and Verdine, G. L. (2005) Structure of a repair enzyme interrogating undamaged DNA elucidates recognition of damaged DNA, *Nature 434*, 612−8.
18. Fromme, J. C., and Verdine, G. L. (2002) Structural insights into lesion recognition and repair by the bacterial 8-oxoguanine DNA glycosylase MutM, *Nat. Struct. Biol. 9*, 544−52.
19. Gilboa, R., Zharkov, D. O., Golan, G., Fernandes, A. S., Gerchman, S. E., Matz, E., Kycia, J. H., Grollman, A. P., and Shoham, G. (2002) Structure of formamidopyrimidine-DNA glycosylase covalently complexed to DNA, *J. Biol. Chem. 277*, 19811−6.
20. Serre, L., Pereira de Jesus, K., Boiteux, S., Zelwer, C., and Castaing, B. (2002) Crystal structure of the *Lactococcus lactis* formamidopyrimidine-DNA glycosylase bound to an abasic site analogue-containing DNA, *EMBO J. 21*, 2854−65.
21. Doublie, S., Bandaru, V., Bond, J. P., and Wallace, S. S. (2004) The crystal structure of human endonuclease VIII-like 1 (NEIL1) reveals a zincless finger motif required for glycosylase activity, *Proc. Natl. Acad. Sci. U.S.A. 101*, 10284−9.
22. Zharkov, D. O., Golan, G., Gilboa, R., Fernandes, A. S., Gerchman, S. E., Kycia, J. H., Rieger, R. A., Grollman, A. P., and Shoham, G. (2002) Structural analysis of an *Escherichia coli* endonuclease VIII covalent reaction intermediate, *EMBO J. 21*, 789−800.
23. Daujotyte, D., Serva, S., Vilkaitis, G., Merkiene, E., Venclovas, C., and Klimasauskas, S. (2004) HhaI DNA methyltransferase uses the protruding Gln237 for active flipping of its target cytosine, *Structure 12*, 1047−55.
24. Jiang, Y. L., Kwon, K., and Stivers, J. T. (2001) Turning On uracil-DNA glycosylase using a pyrene nucleotide switch, *J. Biol. Chem. 276*, 42347−54.
25. Handa, P., Roy, S., and Varshney, U. (2001) The role of leucine 191 of *Escherichia coli* uracil DNA glycosylase in the formation of a highly stable complex with the substrate mimic, ugi, and in uracil excision from the synthetic substrates, *J. Biol. Chem. 276*, 17324−31.
26. Parikh, S. S., Mol, C. D., Slupphaug, G., Bharati, S., Krokan, H. E., and Tainer, J. A. (1998) Base excision repair initiation revealed by crystal structures and binding kinetics of human uracil-DNA glycosylase with DNA, *EMBO J. 17*, 5214−26.
27. Parikh, S. S., Walcher, G., Jones, G. D., Slupphaug, G., Krokan, H. E., Blackburn, G. M., and Tainer, J. A. (2000) Uracil-DNA glycosylase-DNA substrate and product structures: Conformational strain promotes catalytic efficiency by coupled stereoelectronic effects, *Proc. Natl. Acad. Sci. U.S.A. 97*, 5083−8.
28. Guan, Y., Manuel, R. C., Arvai, A. S., Parikh, S. S., Mol, C. D., Miller, J. H., Lloyd, S., and Tainer, J. A. (1998) MutY catalytic core, mutant and bound adenine structures define specificity for DNA repair enzyme superfamily, *Nat. Struct. Biol. 5*, 1058−64.
29. Scharer, O. D., Ortholand, J. Y., Ganesan, A., Ezaz-Nikpay, K., and Verdine, G. L. (1995) Specific binding of the DNA repair enzyme AlkA to a pyrrolidine-based inhibitor, *J. Am. Chem. Soc. 117*, 6623−4.
30. Scharer, O. D., Kawate, T., Gallinari, P., Jiricny, J., and Verdine, G. L. (1997) Investigation of the mechanisms of DNA binding of the human G/T glycosylase using designed inhibitors, *Proc. Natl. Acad. Sci. U.S.A. 94*, 4878−83.
31. McCullough, A. K., Scharer, O., Verdine, G. L., and Lloyd, R. S. (1996) Structural determinants for specific recognition by T4 endonuclease V, *J. Biol. Chem. 271*, 32147−52.
32. Allan, B. W., Reich, N. O., and Beechem, J. M. (1999) Measurement of the absolute temporal coupling between DNA binding and base flipping, *Biochemistry 38*, 5308−14.
33. Gowher, H., and Jeltsch, A. (2000) Molecular enzymology of the EcoRV DNA-(Adenine-N(6))-methyltransferase: Kinetics of DNA binding and bending, kinetic mechanism and linear diffusion of the enzyme on DNA, *J. Mol. Biol. 303*, 93−110.
34. Reddy, Y. V., and Rao, D. N. (2000) Binding of EcoP15I DNA methyltransferase to DNA reveals a large structural distortion within the recognition sequence, *J. Mol. Biol. 298*, 597−610.
35. Wong, I., Lundquist, A. J., Bernards, A. S., and Mosbaugh, D. W. (2002) Presteady-state analysis of a single catalytic turnover by *Escherichia coli* uracil-DNA glycosylase reveals a "pinch-pull-push" mechanism, *J. Biol. Chem. 277*, 19424−32.
36. Stivers, J. T., Pankiewicz, K. W., and Watanabe, K. A. (1999) Kinetic mechanism of damage site recognition and uracil flipping by *Escherichia coli* uracil DNA glycosylase, *Biochemistry 38*, 952−63.
37. Jiang, Y. L., and Stivers, J. T. (2002) Mutational analysis of the base-flipping mechanism of uracil DNA glycosylase, *Biochemistry 41*, 11236−47.
38. Zhao, X., Liu, J., Hsu, D. S., Zhao, S., Taylor, J. S., and Sancar, A. (1997) Reaction mechanism of (6-4) photolyase, *J. Biol. Chem. 272*, 32580−90.
39. Vande Berg, B. J., and Sancar, G. B. (1998) Evidence for dinucleotide flipping by DNA photolyase, *J. Biol. Chem. 273*, 20276−84.
40. Christine, K. S., MacFarlane, A. W. t., Yang, K., and Stanley, R. J. (2002) Cyclobutylpyrimidine dimer base flipping by DNA photolyase, *J. Biol. Chem. 277*, 38339−44.
41. Allan, B. W., Garcia, R., Maegley, K., Mort, J., Wong, D., Lindstrom, W., Beechem, J. M., and Reich, N. O. (1999) DNA bending by EcoRI DNA methyltransferase accelerates base flipping but compromises specificity, *J. Biol. Chem. 274*, 19269−75.
42. Hopkins, B. B., and Reich, N. O. (2004) Simultaneous DNA binding, bending, and base flipping: Evidence for a novel M.EcoRI methyltransferase-DNA complex, *J. Biol. Chem. 279*, 37049−60.
43. Huang, N., Banavali, N. K., and MacKerell, A. D., Jr. (2003) Protein-facilitated base flipping in DNA by cytosine-5-methyltransferase, *Proc. Natl. Acad. Sci. U.S.A. 100*, 68−73.
44. Jaruga, P., Jabil, R., McCullough, A. K., Rodriguez, H., Dizdaroglu, M., and Lloyd, R. S. (2002) Chlorella virus pyrimidine dimer glycosylase excises ultraviolet radiation- and hydroxyl radical-induced products 4,6-diamino-5-formamidopyrimidine and 2,6-diamino-4-hydroxy-5-formamidopyrimidine from DNA, *Photochem. Photobiol. 75*, 85−91.
45. Pace, C. N., Vajdos, F., Fee, L., Grimsley, G., and Gray, T. (1995) How to measure and predict the molar absorption coefficient of a protein, *Protein Sci. 4*, 2411−23.
46. Iakoucheva, L. M., Walker, R. K., van Houten, B., and Ackerman, E. J. (2002) Equilibrium and stop-flow kinetic studies of fluorescently labeled DNA substrates with DNA repair proteins XPA and replication protein A, *Biochemistry 41*, 131−43.
47. Neely, R. K., Daujotyte, D., Grazulis, S., Magennis, S. W., Dryden, D. T., Klimasauskas, S., and Jones, A. C. (2005) Time-resolved fluorescence of 2-aminopurine as a probe of base flipping in M.HhaI-DNA complexes, *Nucleic Acids Res. 33*, 6953−60.
48. Latham, K. A., Manuel, R. C., and Lloyd, R. S. (1995) The interaction of T4 endonuclease V E23Q mutant with thymine dimer- and tetrahydrofuran-containing DNA, *J. Bacteriol. 177*, 5166−8.
49. Cao, C., Jiang, Y. L., Stivers, J. T., and Song, F. (2004) Dynamic opening of DNA during the enzymatic search for a damaged base, *Nat. Struct. Mol. Biol. 11*, 1230−6.
50. Krosky, D. J., Schwarz, F. P., and Stivers, J. T. (2004) Linear free energy correlations for enzymatic base flipping: How do damaged base pairs facilitate specific recognition? *Biochemistry 43*, 4188−95.
51. Krosky, D. J., Song, F., and Stivers, J. T. (2005) The origins of high-affinity enzyme binding to an extrahelical DNA base, *Biochemistry 44*, 5949−59.
52. Banerjee, A., Santos, W. L., and Verdine, G. L. (2006) Structure of a DNA glycosylase searching for lesions, *Science 311*, 1153−7.

BI060802S